Electronic Supplementary Material (ESI) for Chemical Communications.

Supporting Information

Solvatochromism as a probe to observe the solvent exchange process in a 1-D porous coordination polymer with 1-D solvent accessible channels.

Charl X. Bezuidenhout, Catharine Esterhuysen and Leonard J. Barbour*

Department of Chemistry and Polymer Science
University of Stellenbosch
Matieland 7602, South Africa
E-mail: ljb@sun.ac.za

Materials and synthesis

All chemicals were obtained from commercial sources (mainly Sigma Aldrich) and used without further purification. The 3,6-di(pyridin-4-yl)-1,2,4,5-tetrazine (dptz) linker was synthesised according to reported procedures[S1].

Single-crystal X-ray Diffraction

Suitable single-crystals were selected and loaded onto the diffractometer using a MiTeGen MicroCrystal mounts. Single-crystal X-ray diffraction data were collected using a SMART diffractometer with an APEX-II CCD area-detector using an Oxford Cryosystems 700Plus cryostat for temperature control. X-rays were generated from a sealed tube (MoKα radiation λ = 0.71073 Å) fitted with a multilayer monochromator. All data were collected at 100 K.

Data reduction was carried out by means of the standard procedure using the Bruker software package SAINT2 and the absorption corrections and the correction of other systematic errors were performed using SADABS.3. Using Xseed [S2] and Olex2 [S3], the structure was solved with the ShelXS [S4] structure solution program using Direct Methods and refined with the ShelXL [S5] refinement package using least squares minimisation. Hydrogen atoms were placed in calculated positions using riding models.

Thermogravimetric analysis (TGA)

Thermogravimetric analysis was conducted using a TA Instrument Q500. The sample is loaded in an aluminium pan and heated from room temperature at 10 °C/min up to 600°C.

Time-Lapsed Polarized-light Optical Microscopy

Single crystals of the chloroform solvate (**1a**) were immersed in acetonitrile and nitromethane and sealed within a chamber with windows at the top and bottom. Adjustment (lighting, crystal position, polarizer, etc.) were made very quickly and pictures were taken every 10 seconds.

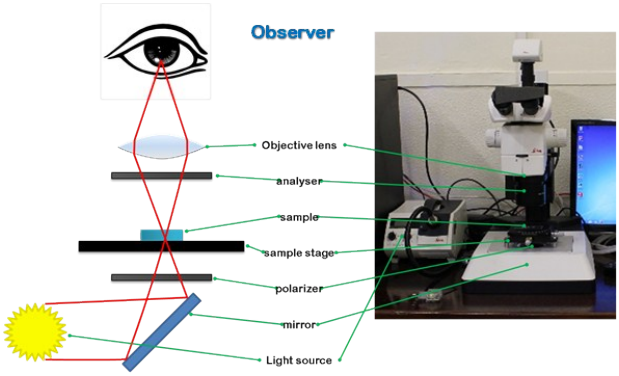

Scheme 1. The Leica optical microscope setup used in the solvent-exchange experiments.

Computational Methods

Geometry Optimizations and Atomic charges

Only the hydrogen atoms of the frameworks are optimized as part of a periodic system using the CASTEP module of the Materials Studio software suite.[S6] The optimization was performed using the GGA PBE functional with Grimme's DFT-D dispersion correction; thresholds for geometry optimization and SCF convergence were chosen as 1×10^{-6} eV. The Milliken charges were calculated at the end of the optimisation process (this is given as an option in the properties tab of the calculation setup). These atomic charges are used in all the subsequent molecular mechanics calculations.

DMol^3 UV-vis calculations

UV-vis data was calculated at the end of the optimization step using the DMol^3 module within the Biovia Materials Studio software suite.[S6-S8] The optimization was performed using the The Perdew et al.[S9] generalized gradient approximation (GGA/PBE) for the exchange–correlation functional [S10] and the dispersion corrected with Grimme's DFT-D. The thresholds for the geometry optimizations and SCF convergence were chosen as 1×10^{-6} eV. An all-electron core treatment with the TNP basis (Triple Numerical plus polarization) was chosen to describe the electronic structure for the organic models and the Effective Core Potentials with a DNP (Double Numerical plus polarization) basis was chosen for the models containing copper cations.[S11] The UV-vis spectra were calculated at the GGA/PBE level using TD-DFT with the ALDA (adiabatic local exchange functional approximation) approach that is recommended by the DMol^3 author as a cost-efficient implementation of TD-DFT.[S12] The TD-DFT excitations were calculated using the **ALDA** kernel with exchange-correlation terms included, other options include: **ALDAx** - calculates TD-DFT excitations using a modified ALDA kernel with the exchange term only; **RPA** - no exchange-correlation response, only electrostatic response included) for calculating the 50 lowest singlet states.[S13, S14] Only the grid data for 10 orbitals above and below the Fermi level were calculated for visualization.

Adsorption calculations

All adsorption calculations were performed using the Adsorption Locator module within the Biovia Materials Studio software suite.[S6] This module allows for the simulation of pure and mixed adsorbates, with fixed composition, onto a substrate. The Adsorption Locator module identifies possible adsorption sites by carrying out Monte Carlo searches of the configurational space of the substrate-adsorbate system as the temperature is slowly decreased within the simulated annealing process of a molecular dynamics run. [S15-S18] In this work we simulated the adsorption of a solvent molecules onto particular crystal facets in order to acquire relative interaction strengths of the different solvents with the different crystal facets. This can provide insight into the facet preferences of solvent exchange processes. The adsorption locator is essentially a simulated annealing simulation with geometry optimizations in-between successive heat-cool cycles. A model several unit cells in size were constructed and cleaved along a plane ([10-2] and (2 1 2)) to create the appropriate crystal face onto which a vacuum slab is added. One hundred adsorbate molecules were introduced into the vacuum as part of the simulated annealing calculation. The isosteric heat, or enthalpy of adsorption, can be extracted from the adsorption calculation and is an average over all the lowest energy configurations (obtained using Monte Carlo simulations) returned after each annealing cycle of the MD run. 30 cycles containing 1 000 000 steps per cycle with annealing temperatures of 298 to 500 K were used for reproducible results. The Monte Carlo parameters were set to a probability of 0.29 (ratio = 1) for 'conformer', 'rotate' and 'translate' while 'regrow' was set to 0.14 (ratio = 0.5). The

COMPASS force field (COMPASS II 1.0)[S19] was used in conjunction with atomic charges calculated using CASTEP single point energy calculations. Ewald and group based summation methods were chosen for the electrostatic and van der Waals energy components respectively with the cut-off's set at 25 Å. The parameterisation and validation of COMPASS for metal oxides was performed by Zhao and co-workers. [S20] The list of models covered by the COMPASS II 1.0 force field is given below:

Table S1. All the models covered by the COMPASS II 1.0 force field.

COMPASS II 1.0 - Group A - Covalent Model			
Alkanes	C_nH_{2n+2}	Carbamates/urethanes	-OCONH-
Alkenes	C_nH_{2n}	Siloxanes	-Si-O-Si-
Alkynes	C_nH_n	Silanes	-Si-Si-
Benzenes/Aromatics	C_6H_6, $-C_6H_5$, $C_{12}H_{10}$	Small molecules	O_2, N_2, H_2, H_2O, CO, CO_2, CS_2, SO_2, SO_3, NO, NO_2, NH_3, He, Ne, Ar, Kr, Xe
Cycloalkanes	C_nH_{2n}	Alkyl halides	R-X (X=F, Cl)
Ethers	-R-O-R-	Phosphazenes	$-N=PX_2-$ (X=F, Cl, NR, OR, R)
Acetals	$-C(OR)_2-$	Nitro groups	$-NO_2$
Alcohols	-R-OH	Nitriles	R-CN
Phenols	Ar-OH	Isocyanides	RNCO
Amines	$-NR_2$	Sulfides	RSR
Ammonia	NH_3	Thiols	RSH
Aldehyde/ketone	-CO-	Amineoxides	NR_3O
Acids	-COOH	Aromatic halides	Ar-Cl, Ar-F
Esters	-COO-	Cyanamides	-N=C=O
Carbonates	-OCOO-	Nitrates	$R-O-NO_2$
Amides	-CONH-	Sulfates	$-SO_4-$
		Sulfonates	RSO_2O-
COMPASS II 1.0 - Group B - Ionic Model			
Metals	Al, Na, Pt, Pd, Au, Ag, Sn, K, Li, Mo, Fe, W, Ni, Cr, Cu, Pb, Mg		
Metal halides	Li^+, Na^+, K^+, Rb^+, Cs^+, Mg^{2+}, Ca^{2+}, Fe^{2+}, Cu^{2+}, Zn^{2+}, F^-, Cl^-, Br^-, I^-		
Silica/Aluminosilicates	SiO_2, AlO_2		
Metal oxides	Li_2O, Na_2O, K_2O, MgO, CaO, SrO, BaO, TiO_2, Fe_2O_3, Al_2O_3, SnO_2, SiO_2, CuO		

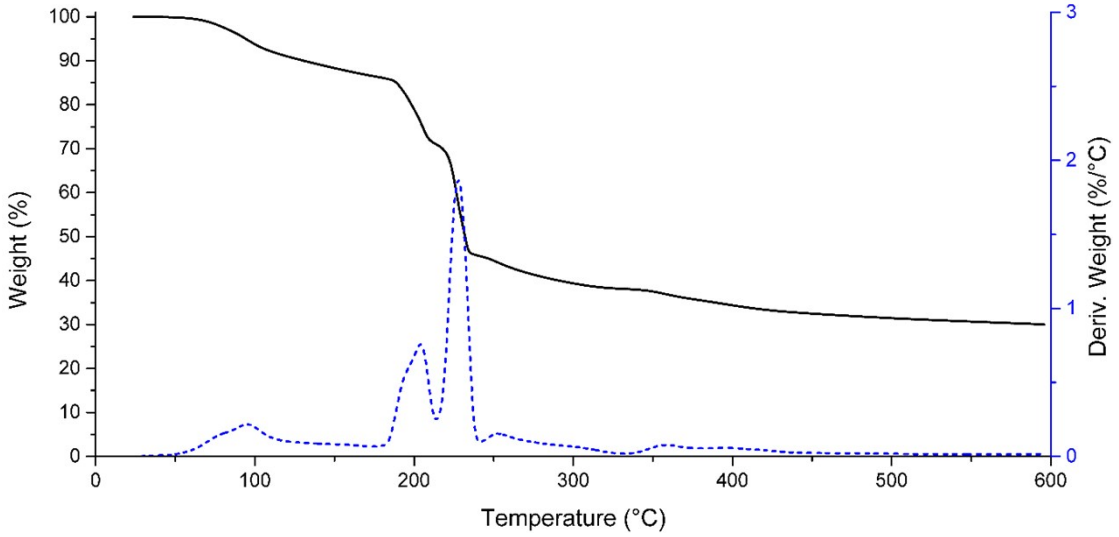

Fig. S1 TGA of **1a** from RT to 600 °C.

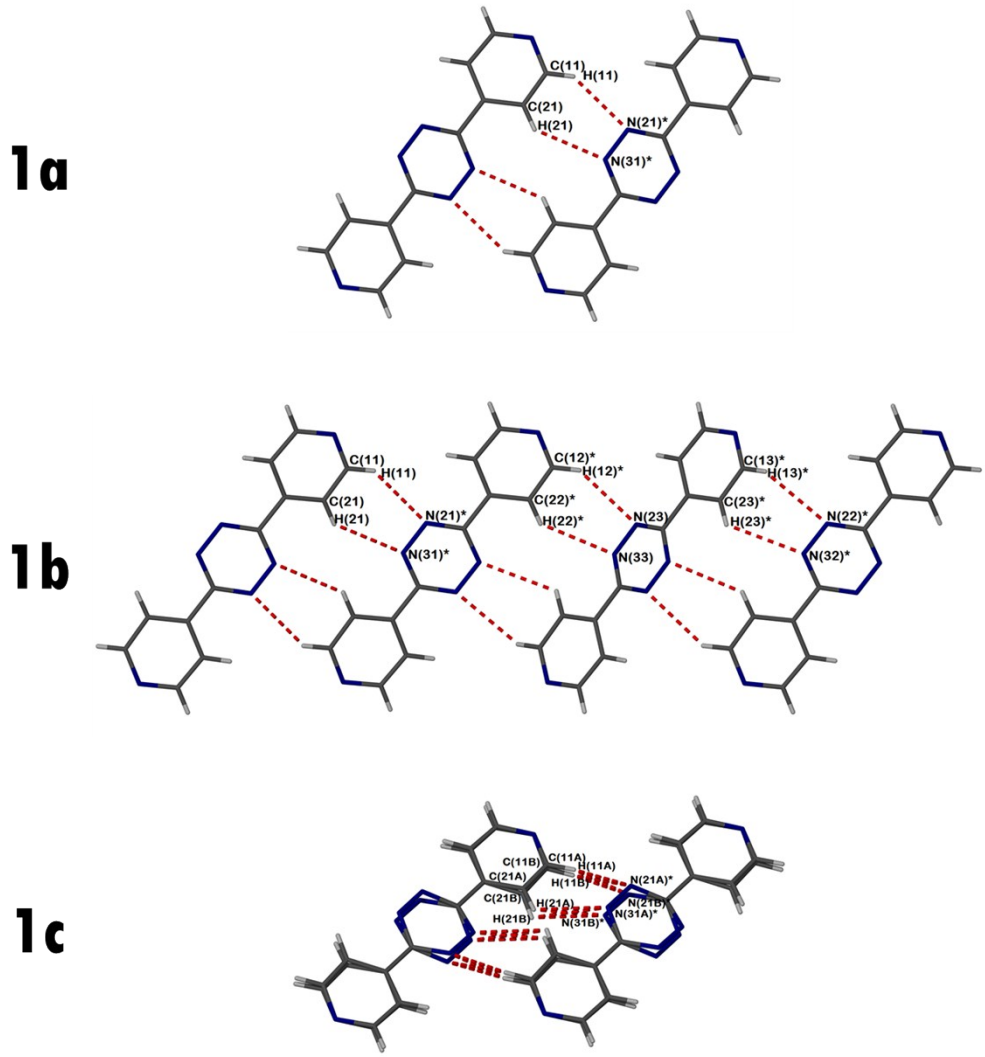

Fig. S2. The C—H···N contacts for the dptz ligands of **1a**, **1b** and **1c**.

Table S2. C—H···N contacts for the dptz ligands of **1a**, **1b** and **1c**.

	D—H···A	Distance (D—A)	Angle (D—H···A)
1a	C(11)—H(11)···N(21)*	3.469(2)	142.52
	C(21)—H(21)···N(31)*	3.440(2)	134.87
1b	C(11)—H(11)···N(21)*	3.494(4)	126.14
	C(12)*—H(12)*···N(23)	3.573(4)	139.76
	C(13)*—H(13)*···N(22)*	3.518(4)	128.97
	C(21)—H(21)···N(31)*	3.481(4)	117.14
	C(22)*—H(22)*···N(33)	3.547(4)	130.97
	C(23)*—H(23)*···N(32)*	3.475(4)	122.26
1c ($A_{S.O.F}$– 0.6301) ($B_{S.O.F}$– 0.3699)	C(11A)—H(11A)···N(21A)*	3.595(6)	124.50
	C(11A)—H(11A)···N(21B)*	3.382(6)	127.54
	C(11B)—H(11B)···N(21A)*	3.677(6)	112.06
	C(11B)—H(11B)···N(21B)*	3.437(6)	116.02
	C(21A)—H(21A)···N(31A)*	3.602(6)	135.61
	C(21A)—H(21A)···N(31B)*	3.372(6)	141.20
	C(21B)—H(21B)···N(31A)*	3.689(6)	124.84
	C(21B)—H(21B)···N(31B)*	3.429(6)	131.00

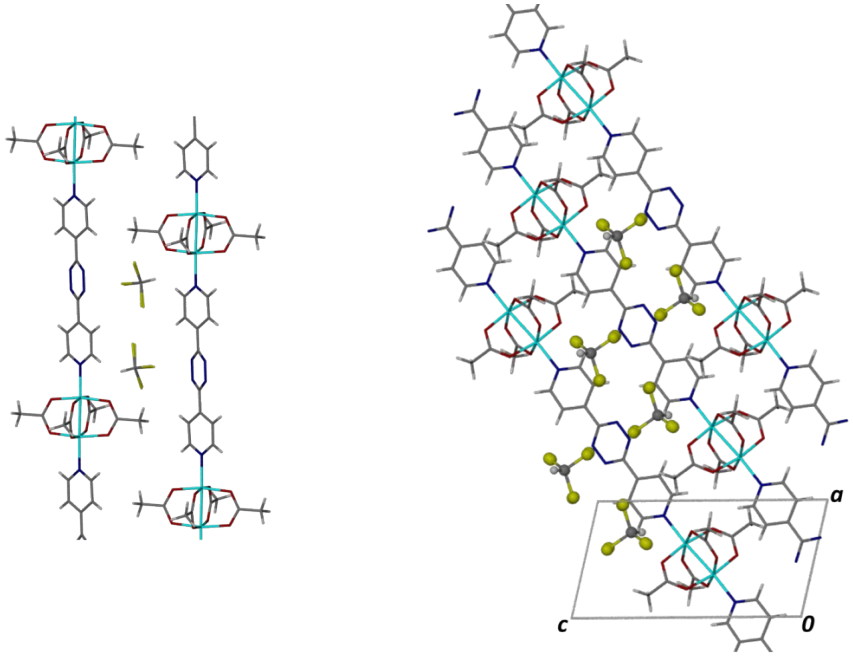

Fig. S3 The interactions of chloroform with the dptz linkers in **1a**.

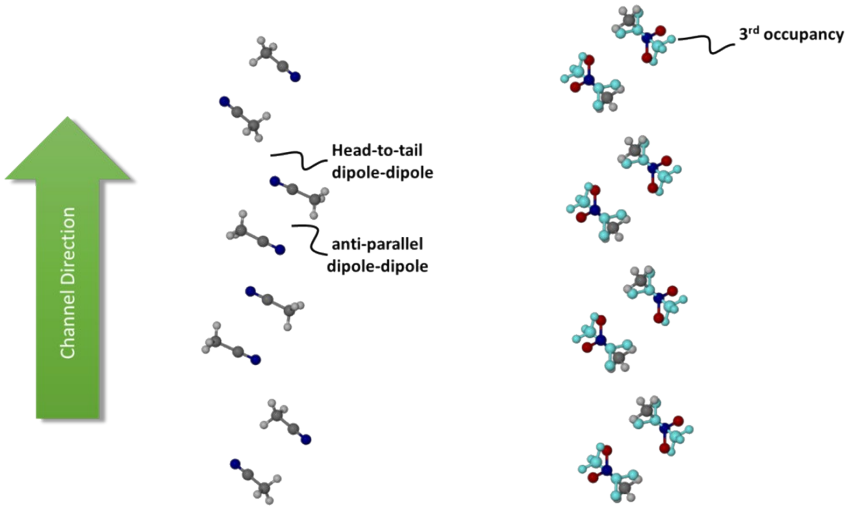

Fig. S4 Left – the acetonitrile guest molecule arrangement within the 1D channel with the channel direction along [0 1 1]. Right – disordered nitromethane which can also form head-to-tail and anti-parallel dipole-dipole interactions (channel direction along [1 0 0]).

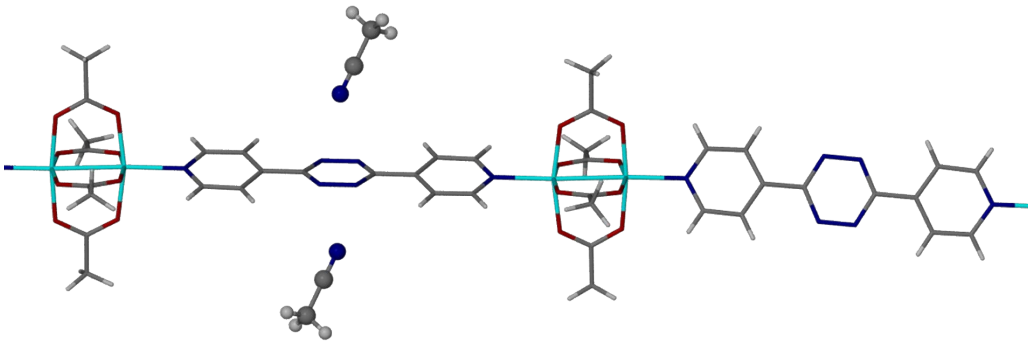

Fig. S5 Head-on interaction of acetonitrile molecules with every 3rd out-of-plane twisted dptz linker.

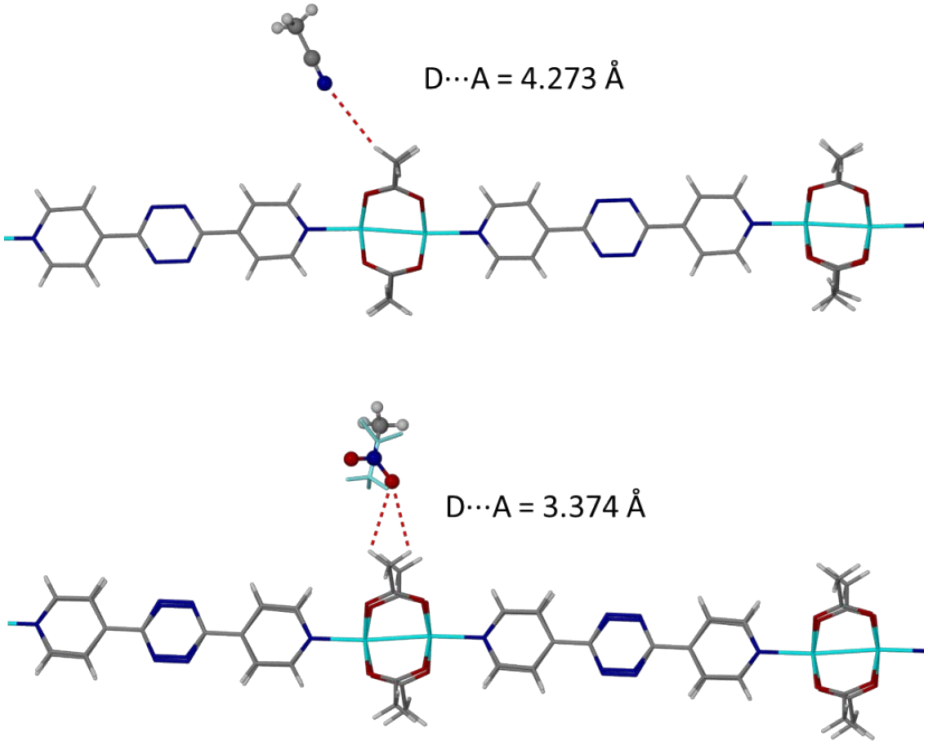

Fig. S6 The hydrogen bonding (electrostatic interaction) of acetonitrile and nitromethane with the methyl-group of the acetate moiety.

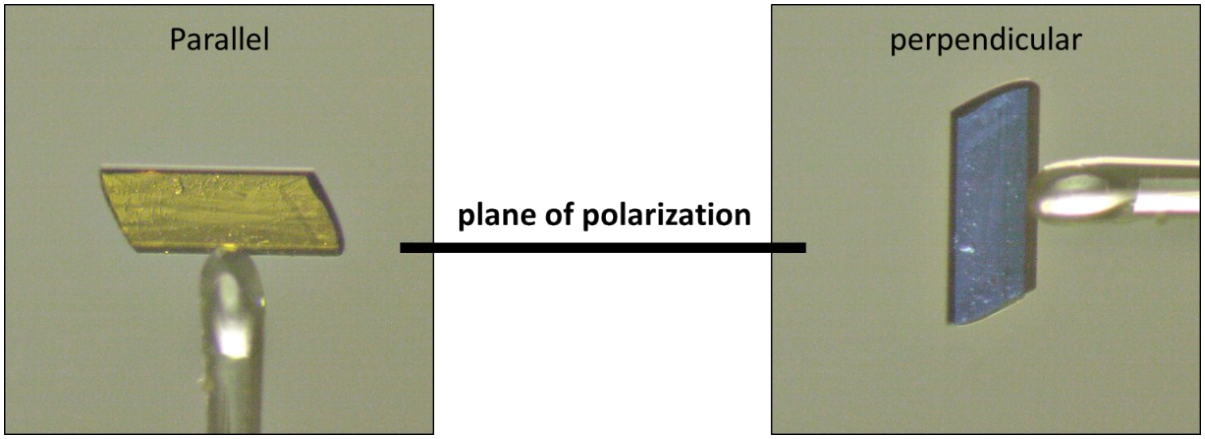

Fig. S7 The colour of a **1a** single crystal parallel and normal to the plane of polarization as viewed through an optical microscope.

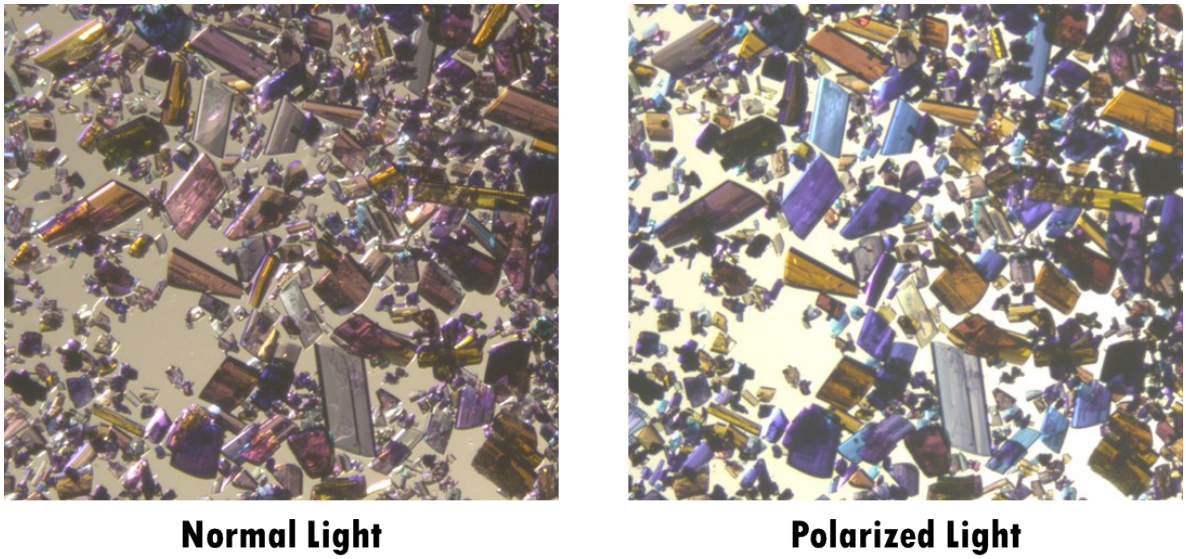

Fig. S8 Left - Crystals of **1a** viewed without a polarizer (the mirror at the bottom of the microscope could slightly polarize the light). Right – Crystals of **1a** viewed with polarized light showing the colour enhancement. The colour of the crystals vary depending on the orientation of the crystals thus illustrating the pleochroism of **1a**.

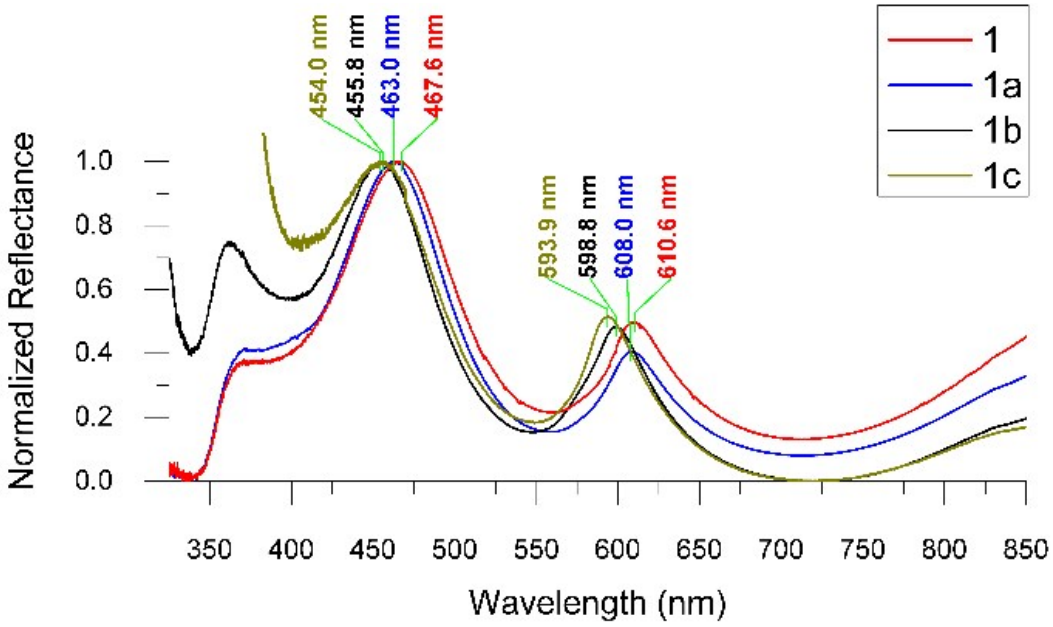

Fig. S9 Normalized reflectance UV-vis spectra of the activated PCP and the three solvates. The peaks of interest are indicated with the green lines.

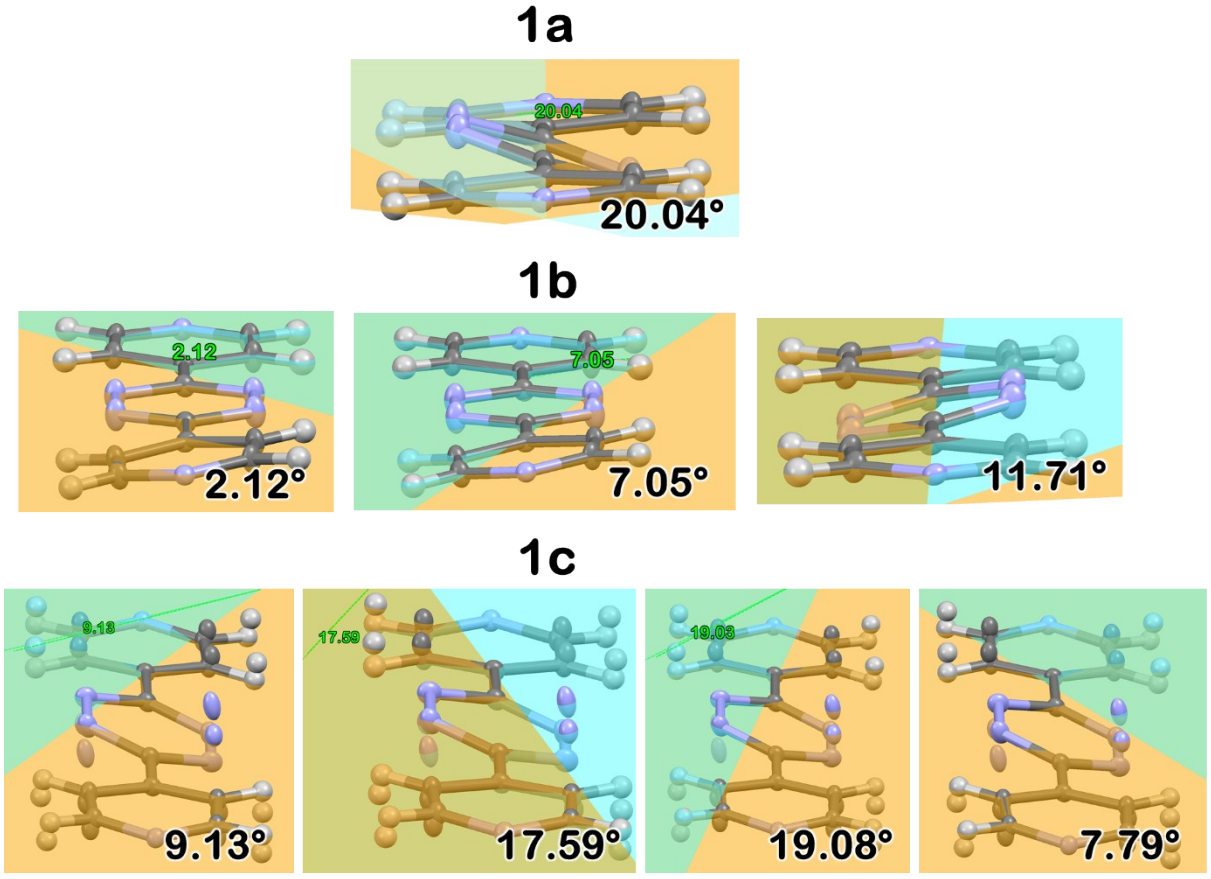

Fig. S10 The tilt angles between the tetrazine and pyridyl rings measured using the Mercury 3.7 software.[S21]

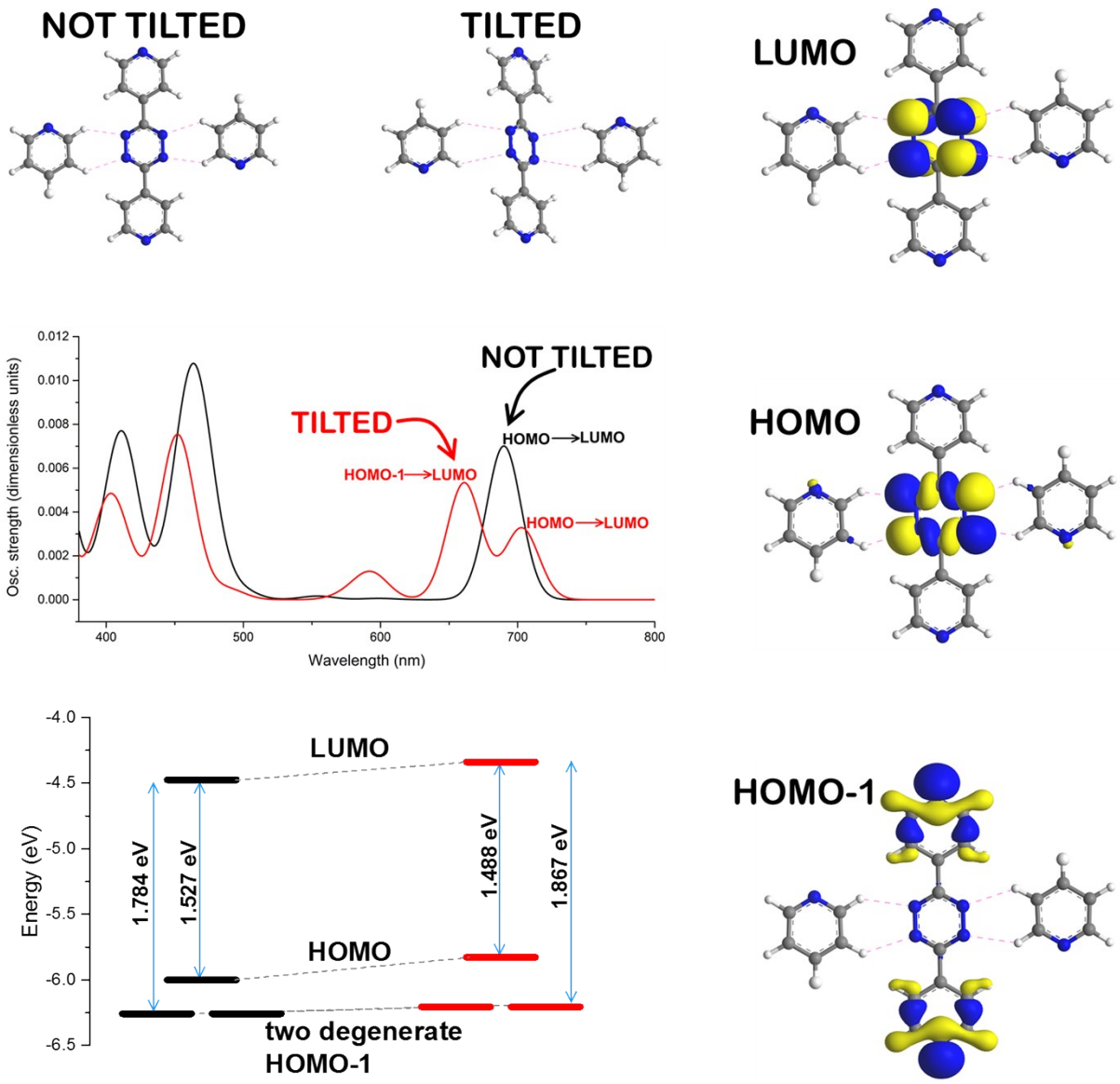

Fig. S11. UV-vis calculations using a single dptz molecule surrounded by 2 pyridine molecules forming C–H···N electrostatic interactions. The dptz molecule was tilted by 45° with respect to its original orientation. The UV-vis spectra and frontier orbitals was calculated for both scenarios. Bottom-Left: the energy diagram for the frontier orbitals. Left: visualization of the frontier orbitals of interest. These calculation was performed using the DMol^3 module in the Materials Studio software package.[S6]

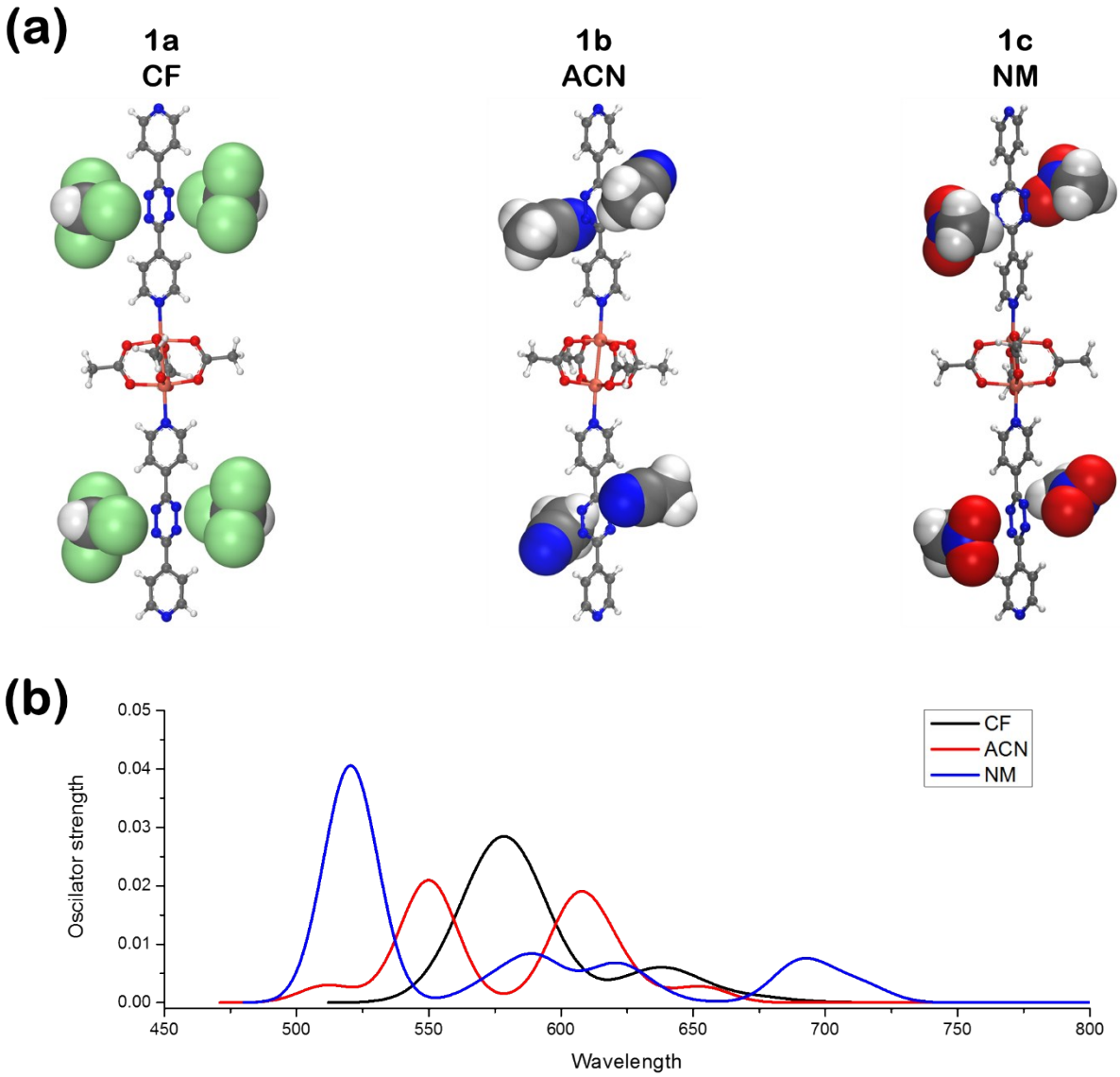

Fig. S12. UV-vis calculations using a paddlewheel moiety with two coordinated dptz linkers and the three solvents. (a) The computational models used for the UV-vis calculations. The solvent molecules is shown in space filling representation. (b) The UV-vis absorption spectra generated using these models. These calculation was performed using the DMol^3 module in the Materials Studio software package.[S6]

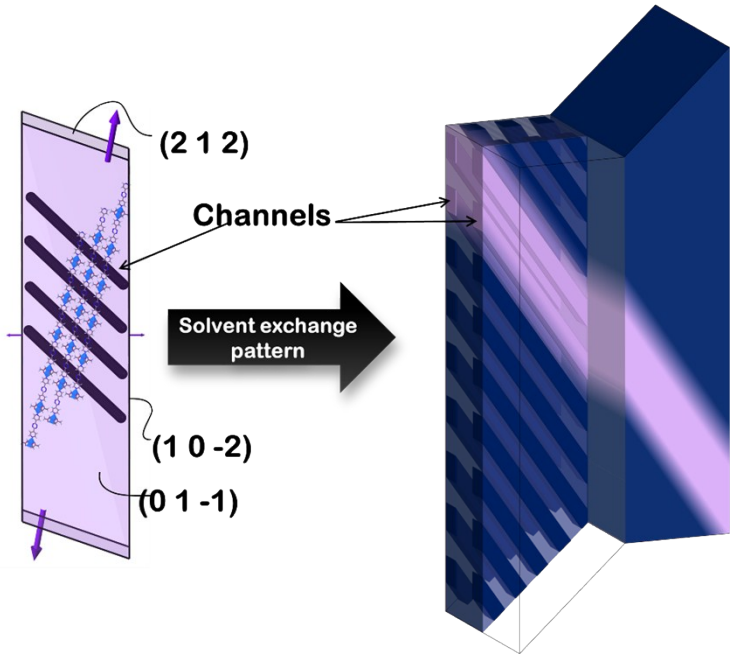

Fig. S13. Left: Overlay of the crystal structure and crystal habit with the channels and facets indicated. Right: Tthe resulting solvent exchange pattern of a single crystal with channels as shown in the overlay. The size and direction of the purple arrows indicate the growth rate of the facets.

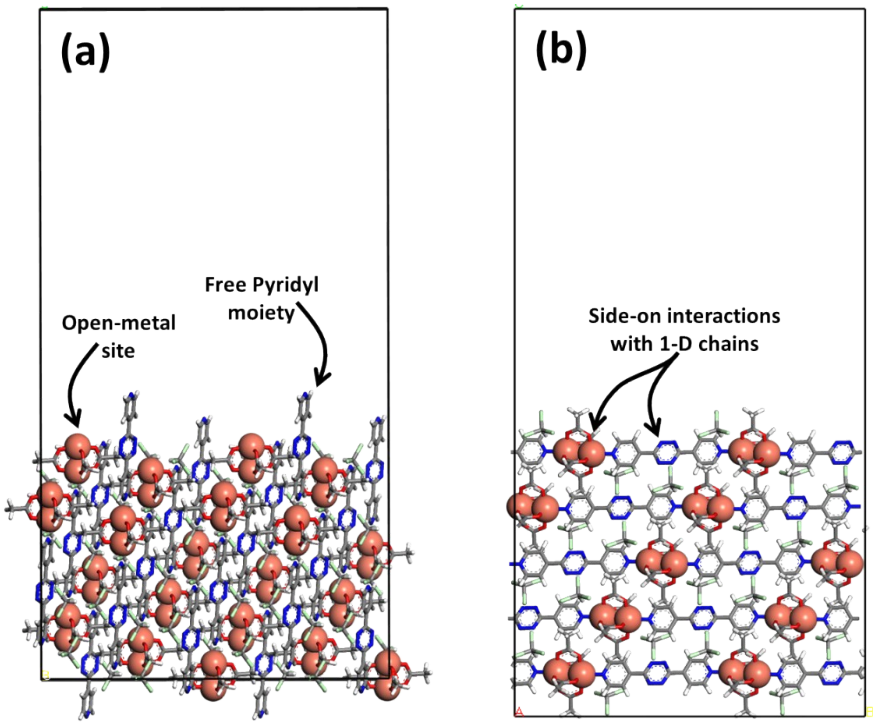

Fig. S14. The models used for the Adsorption Locator simulations with the copper atoms shown in space-filling representation and the rest of the model shown in stick representation. (a) (212) and (b) (10-2).

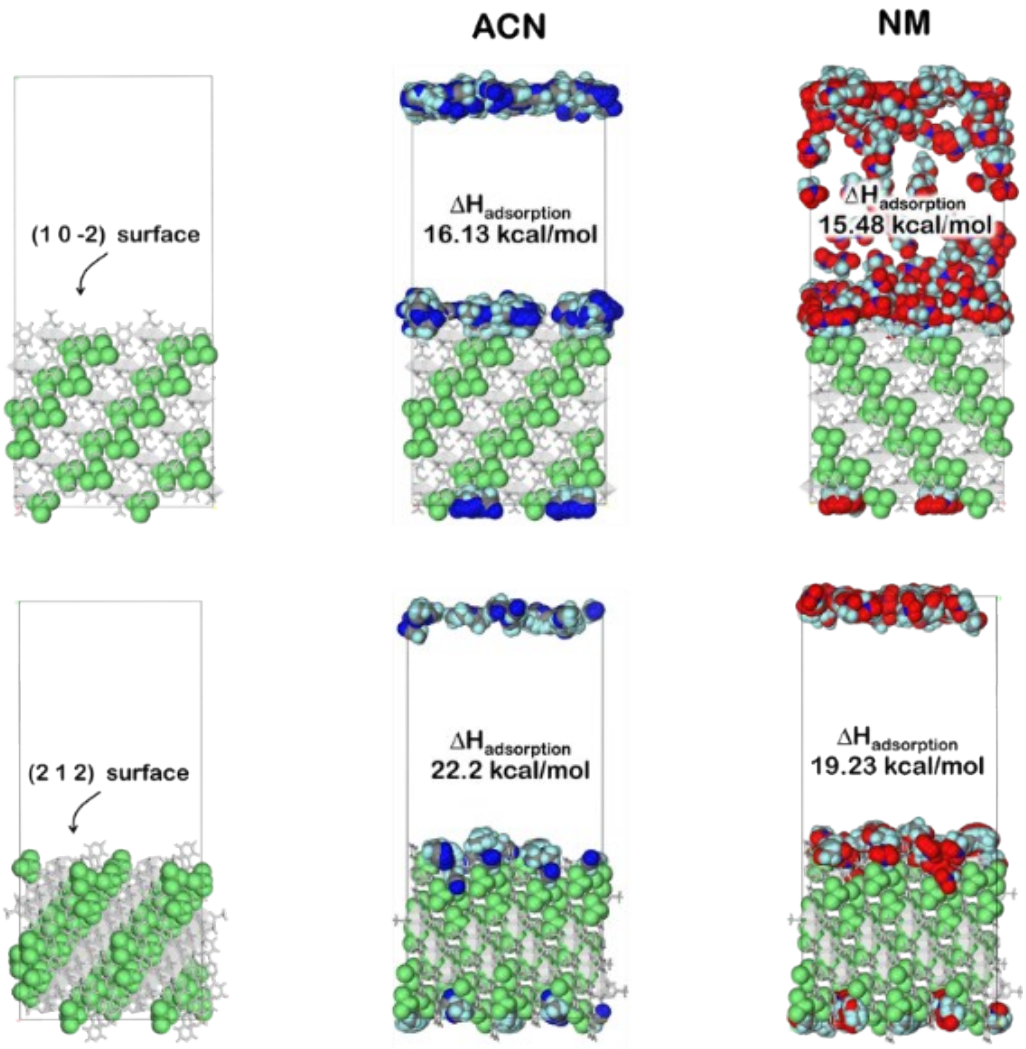

Fig. S15. Left – Molecular Mechanics models used to perform adsorption simulations of ACN and NM onto the (10-2) and (212) surfaces of a crystal of **1a**. Middle – ACN adsorption. Right – NM adsorption. Several snapshots were combined to produce the solvent-containing figures. Solvent molecules are represented in space-fill format and the coordination polymer in grey stick representation.

References

[1] Bakkali, H., et al., *Eur. J. Org. Chem.* **2008**, *2008*, 2156-2166

[2] (a) Atwood, J. L.; Barbour, L. J., *Cryst. Growth Des.* **2003**, *3*, 3-8; (b) Barbour, L. J., *J. Supramol. Chem.* **2001**, *1*, 189-191.

[3] Dolomanov, O.V., Bourhis, L.J., Gildea, R.J, Howard, J.A.K. & Puschmann, H.*, J. Appl. Cryst.* **2009**, *42*, 339-341.

[4] Sheldrick, G.M., *Acta Cryst.* **2008***, A64*, 112-122.

[5] Sheldrick, G.M., *Acta Cryst.* **2015**, *C71*, 3-8.

[6] Materials Studio Modeling Environment v7.0.0; Accelrys Software Inc.: San Diego, **2015**

[7] Delley, B., *J. Chem. Phys.* **1990**, *92*, 508-517.

[8] Delley, B., *J. Chem. Phys.* **2000**, *113*, 7756-7764.

[9] Perdew, J. P.; Burke, K.; Ernzerhof, M., *Phys. Rev. Lett.* **1996**, *77*, 3865-3868.

[10] Chen, F.; Johnston, R. L., *Acta Mater.* **2008**, *56*, 2374-2380.

[11] Inada, Y.; Orita, H., *J. Comput. Chem.* **2008**, *29*, 225-232.

[12] Delley, B., *J. Phys.: Condens. Matter* **2010**, *22*, 384208

[13] Vasiliev, I.; Öğüt, S.; Chelikowsky, J. R., *Phys. Rev. B* **2002**, *65*, 115416.

[14] Li, W.-Y.; Chen, F.-Y., *Chinese Physics B* **2014**, *23*, 117103.

[15] Metropolis, N.; Rosenbluth, A. W.; Rosenbluth, M. N.; Teller, A. H.; Teller, E., *J. Chem. Phys.* **1953**, *21*, 1087-1092.

[16] Kirkpatrick, S.; Gelatt, C. D.; Vecchi, M. P., *Science* **1983**, *220*, 671-680.

[17] Černý, V., *Journal of Optimization Theory and Applications* **1985**, *45*, 41-51.

[18] Frenkel, D.; Smit, B., *Understanding Molecular Simulation: From Algorithms to Applications*. Elsevier Science: 2001.

[19] Peng, Z.; Ewig, C. S.; Hwang, M.-J.; Waldman, M.; Hagler, A. T., *J. Phys. Chem. A* **1997**, *101*, 7243-7252.

[20] Zhao, L.; Liu, L.; Sun, H., *J. Phys. Chem. C* **2007**, *111*, 10610-10617.

[21] Macrae, C. F.; Bruno, I. J.; Chisholm, J. A.; Edgington, P. R.; McCabe, P.; Pidcock, E.; Rodriguez-Monge, L.; Taylor, R.; van de Streek, J.; Wood, P. A., *J. Appl. Crystallogr.* **2008**, *41*, 466-470.